Article

Large exTTF-Based Dendrimers. Self-Assembly and Peripheral Cooperative Multiencapsulation of C

Gustavo Ferna#ndez, Luis Sa#nchez, Emilio M. Pe#rez, and Nazario Marti#n

J. Am. Chem. Soc., **2008**, 130 (32), 10674-10683 • DOI: 10.1021/ja8018498 • Publication Date (Web): 17 July 2008

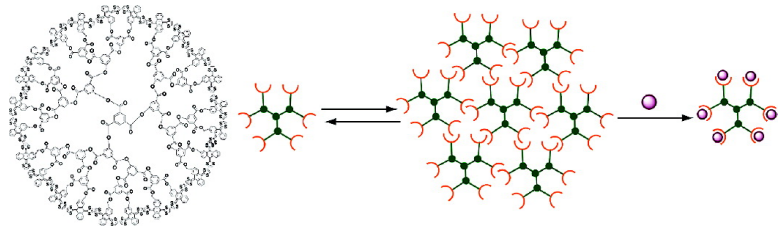

J|A|C|S
ARTICLES

Published on Web 07/17/2008

Large exTTF-Based Dendrimers. Self-Assembly and Peripheral Cooperative Multiencapsulation of C_{60}

Gustavo Fernández,[†] Luis Sánchez,[†] Emilio M. Pérez,[†] and Nazario Martín*[,†,‡]

Departamento de Química Orgánica, Facultad de Química, Universidad Complutense, E-28040 Madrid, Spain and IMDEA-Nanociencia, E-28049 Madrid, Spain

Received March 12, 2008; E-mail: nazmar@quim.ucm.es

Abstract: The convergent synthesis of large monodisperse dendrimers, up to the fourth generation, decorated in their periphery with π-extended tetrathiafulvalene units is reported, and their redox and supramolecular properties are investigated. A number of experiments (MALDI-TOF, ^{1}H NMR at variable temperature and different concentration, DLS, AFM and SEM imaging) confirm the self-aggregation process of these dendrimers, despite the butterfly-like shape of the exTTF units, highly distorted from planarity, to form large supramolecular architectures in the gas phase, in solution, and on a mica surface. Dendrimers **5**, **9**, and **12** host a number of C_{60} molecules to form segregated arrays of donor and acceptor units which could give rise to valuable materials useful for the preparation of optoelectronic devices. UV−vis titration experiments demonstrate that complexation of C_{60} occurs in a positive cooperative manner. Cyclic voltammetry experiments show that the peripheral exTTF units are involved in multioxidation processes. The self-diffusion coefficients (*D*) of the dendrimers reported herein and the previously reported exTTF (**1**) and tweezer (**2**) have been calculated from their chronoamperograms at different concentrations and by the Cottrell equation and, where possible, by PFG-NMR. The calculated values for *D* demonstrate the decrease of this magnitude with increasing dendrimer size.

Introduction

Dendrimers are defined as branched monodisperse polymers,[1] which have been utilized as building blocks in a number of research fields like molecular recognition and inclusion,[2] catalysis,[3] dendronized polymers for the preparation of devices,[4] and drug release.[5] In addition, a number of dendrimers decorated in their focal center, in their periphery or in their branches with redox-active groups, like metalloporphyrins,[6] ferrocene,[7] fullerenes,[8] or tetrathiafulvalenes,[9] among others,[10] have found applications as diverse as providing insight into the dynamics of electron transport at surfaces and within restricted reaction spaces; the preparation of new materials for energy conversion; organic semiconductors and magnets; and the synthesis of artificial systems resembling biological redox processes.[11] Regarding their structure, dendrimers are able to adopt a (pseudo)globular shape as a result of the control that can be exerted over their size and molecular architectures. Besides that, dendrimers are known to self-assemble, typically by means of noncovalent interactions, giving rise to dynamic materials

[†] Universidad Complutense.
[‡] IMDEA-Nanociencia.

(1) (a) Fréchet, J. M. J.; Tomalia, D. A. *Dendrimers and Other Dendritic Polymers*; VCH-Wiley: New York, 2000. (b) Newkome, G. R.; Moorefield, C. N.; Vögtle, F. *Dendrimers and Dendrons: Concepts, Syntheses, Applications*; Wiley-VCH: Weinheim, 2001. (c) Grayson, S. M.; Fréchet, J. M. J. *Chem. Rev.* **2001**, *101*, 3819–3867. (d) Helms, B.; Meijer, E. W. *Science* **2006**, *313*, 929–930.

(2) (a) Chang, T.; Pieterse, K.; Broeren, M. A. C.; Kooijman, H.; Spek, A. L.; Hilbers, P. A. J.; Meijer, E. W. *Chem.—Eur. J.* **2007**, *13*, 7883–7889. (b) Li, W.-S.; Jiang, D.-L.; Suna, Y.; Aida, T. *J. Am. Chem. Soc.* **2005**, *127*, 7700–7702. (c) Epperson, J. D.; Ming, L.-J.; Baker, G. R.; Newkome, G. R. *J. Am. Chem. Soc.* **2001**, *123*, 8583–8592. (d) Gorman, C. B.; Smith, J. C. *Acc. Chem. Res.* **2001**, *34*, 60–71. (e) Zeng, F.; Zimmerman, S. C. *Chem. Rev.* **1997**, *97*, 1681–1712.

(3) (a) Yamamoto, K.; Kawana, Y.; Tsuji, M.; Hayashi, M.; Imaoka, T. *J. Am. Chem. Soc.* **2007**, *129*, 9256–9257. (b) Diallo, A. K.; Ornelas, C.; Salmon, L.; Ruiz Aranzaes, J.; Astruc, D. *Angew. Chem., Int. Ed.* **2007**, *46*, 8644–8648. (c) Delort, E.; Darbre, T.; Reymond, J. L. *J. Am. Chem. Soc.* **2004**, *126*, 15642–15643. (d) Oosterom, G. E.; Reek, J. N. H.; Kamer, P. C. J.; van Leeuwen, P. W. N. M. *Angew. Chem., Int. Ed.* **2001**, *40*, 1828–1849.

(4) (a) Rajaram, S.; Choi, L.; Rolandi, M.; Fréchet, J. M. *J. Am. Chem. Soc.* **2007**, *129*, 9619–9621. (b) Schüter, A. D. *Top. Curr. Chem.* **2005**, *245*, 151–191. (c) Frauenrath, H. *Prog. Polym. Sci.* **2005**, *30*, 325–384. (d) Li, W.-S.; Jiang, D.-L.; Aida, T. *Angew. Chem., Int. Ed.* **2004**, *43*, 2943–2947. (e) Shu, L.; Schlüter, A. D.; Ecker, C.; Severin, N.; Rabe, J. P. *Angew. Chem., Int. Ed.* **2001**, *40*, 4666–4669.

(5) (a) Gingras, M.; Raimundo, J. M.; Chabre, Y. M. *Angew. Chem., Int. Ed.* **2007**, *46*, 1010–1017. (b) Stiriba, S. E.; Frey, H.; Haag, R. *Angew. Chem., Int. Ed.* **2002**, *41*, 1329–1334. (c) Patri, A. K.; Majoros, I. J.; Baker, J. R., Jr. *Curr. Opin. Chem. Biol* **2002**, *6*, 466–471. (d) Astruc, D.; Chardac, F. *Chem. Rev.* **2001**, *101*, 2991–3024.

(6) (a) Tsuda, A.; Alam, M. A.; Harada, T.; Yamaguchi, T.; Ishii, N.; Aida, T. *Angew. Chem., Int. Ed.* **2007**, *46*, 8198–8202. (b) Li, W.-S.; Jiang, D.-L.; Suna, Y.; Aida, T. *J. Am. Chem. Soc.* **2005**, *127*, 7700–7702.

(7) (a) Cardona, C. M.; Kaifer, A. E. *J. Am. Chem. Soc.* **1998**, *120*, 4023–4024. (b) Nijhuis, C. A.; Huskens, J.; Reinhoudt, D. N. *J. Am. Chem. Soc.* **2004**, *126*, 12266–12267.

(8) (a) Hahn, U.; Maisonhaute, E.; Amatore, C.; Nierengarten, J.-F. *Angew. Chem., Int. Ed.* **2007**, *46*, 951–954. (b) El-Khouly, M. E.; Kang, E. S.; Kay, K.-Y.; Choi, C. S.; Aaraki, Y.; Ito, O. *Chem.—Eur. J.* **2007**, *13*, 2854–2863.

(9) (a) Bryce, M. R.; Devonport, W.; Moore, A. J. *Angew. Chem., Int. Ed. Engl.* **1994**, *33*, 1761–1763. (b) Christensen, C. A.; Becher, J.; Goldenberg, L. M.; Bryce, M. R. *Chem. Commun.* **1998**, 509–510. (c) Godbert, N.; Bryce, M. R. *J. Mater. Chem.* **2002**, *12*, 27–36.

(10) (a) Guldi, D. M.; Swartz, A.; Luo, C.; Gómez, R.; Segura, J. L.; Martín, N. *J. Am. Chem. Soc.* **2002**, *124*, 10875–10886. (b) Segura, J. L.; Gómez, R.; Martín, N.; Luo, C.; Swartz, A.; Guldi, D. M. *Chem. Commun.* **2001**, 707–708.

10.1021/ja8018498 CCC: $40.75

capable of responding to external stimuli.[12] They are also able to rearrange to accommodate inclusion guests and, as result of this complexation process, vary their intrinsic shape and function.[13] All the above features place dendrimers in a privileged position for their use in the bottom-up approach to nanoscience.[14]

The interaction among electroactive organic molecules by means of weak forces provokes their organization at the nanoscopic level and allows the correct operation of natural and artificial systems, like the photosynthetic apparatus in plants and bacteria and organic electronics.[15,16] Different approaches have been utilized to achieve a controlled self-assembly of a variety of electron donor (D) and electron acceptor (A) units, ranging from supramolecular dyads and triads to more complex systems like polymers, rosettes, etc.[17] These approaches rely on arrays of H-bonds,[18] metal coordination,[19] or solvophobic interactions[20] as the noncovalent forces responsible for joining the electroactive counterparts.

Recently, we have harnessed the complementary geometrical and electronic features of the electron donor 2-[9-(1,3-dithiol-2-ylidene)anthracen-10(9*H*)-ylidene]-1,3-dithiole (exTTF), a well-known π-extended analogue of tetrathiafulvalene,[21] and related analogues to prepare supramolecular partners for the electron acceptor C_{60}.[22,23a,b] This approach leads to dimers, polymers, or dynamically polydisperse dendrimers, in which $\pi-\pi$ aromatic interactions are responsible for the complexation process.[23c,d] In addition, the combination of these electroactive units, either in a covalent or in a supramolecular fashion, has proven to undergo efficient photoinduced electron transfer processes leading to long-lived radical pairs.[24]

Herein, we report on the synthesis and redox properties of a set of dendrimers, from generation two to generation four, decorated with exTTF units as dendritic head groups. The dendrimers reported in this work have been demonstrated to self-assemble by $\pi-\pi$ aromatic interactions by means of mass spectrometry, ^{1}H NMR experiments at different concentrations and variable temperature, UV−vis spectroscopy, dynamic light scattering (DLS), and AFM and SEM imaging. In addition, the dense outward portion of concave exTTF fragments allows them to act as polyvalent receptors for C_{60}, thus creating segregated arrays of multiple D and A units on their surface. As zeroth and first generations, we have considered the previously reported pristine exTTF[25] (compound **1** in Scheme 1) and the tweezer (**2**),[23a] in which two exTTF moieties are connected by an isophthalic diester unit.

Results and Discussion

Synthesis and Characterization. The synthesis of the multi-exTTF dendrimers has been carried out following a convergent strategy[1c] from dendron **3**, previously reported by our research group[23c] (Scheme 1). For the synthesis of G2 and G3 dendrimers (compounds **5** and **9**) we have followed an analogous protocol to that reported by Godbert and Bryce for related dendrimers.[9c] The G2 dendrimer has been prepared by using a 3-fold esterification reaction of dendron **3** with the commercially available benzene-1,3,5-tricarboxylic acid chloride (**4**) to afford **5** in 77% yield.

The synthesis of G3 dendrimer **9**, obtained in a 53% yield, requires the sequential esterification reaction of dendron **3** with the *tert*-butyldimethylsilyl protected diacid chloride **6**,[26] further

(11) (a) Ma, C.-Q.; Mena-Osteritz, E.; Debaerdemaeker, T.; Wienk, M. M.; Janssen, R. A. J.; Bäuerle, P. *Angew. Chem., Int. Ed.* **2007**, *46*, 1679–1683. (b) Burn, P. L.; Lo, S.-C.; Samuel, I. D. W. *Adv. Mater.* **2007**, *19*, 1675–1688. (c) Li, W.-S.; Kim, K. S.; Jiang, D.-L.; Tanaka, H.; Kawai, T.; Kwon, J. H.; Kim, D.; Aida, T. *J. Am. Chem. Soc.* **2006**, *128*, 10527–10532. (d) Thomas, K. R. J.; Thompson, A. L.; Sivakumar, A. V.; Bardeen, C. J.; Thayumanavan, S. *J. Am. Chem. Soc.* **2005**, *127*, 373–383. (e) Percec, V.; Glodde, M.; Bera, T. K.; Miura, Y.; Shiyanovskaya, I.; Singer, K. D.; Balagurusamy, V. S. K.; Heiney, P. A.; Schnell, I.; Rapp, A.; Spiess, H.-W.; Hudsonk, S. D.; Duank, H. *Nature* **2002**, *419*, 384–387.

(12) (a) Franz, A.; Bauer, W.; Hirsch, A. *Angew. Chem., Int. Ed.* **2005**, *44*, 1564–1567. (b) Kellermann, M.; Bauer, W.; Hirsch, A.; Schade, B.; Ludwig, K.; Böttcher, C. *Angew. Chem., Int. Ed.* **2004**, *43*, 2959–2962. (c) Dirksen, A.; Hahn, U.; Schwanke, F.; Nieger, M.; Reek, J. N. H.; Vögtle, F.; De Cola, L. *Chem.—Eur. J.* **2004**, *10*, 2036–2047. (d) Ma, Y. M.; Kolotuchin, S. V.; Zimmerman, S. C. *J. Am. Chem. Soc.* **2002**, *124*, 13757–13769.

(13) (a) Fréchet, J. M. J. *Proc. Natl. Acad. Sci. U.S.A.* **2002**, *99*, 4782–4787. (b) Hecht, S.; Fréchet, J. M. J. *Angew. Chem., Int. Ed.* **2001**, *40*, 74–91.

(14) (a) Lehn, J.-M. *Science* **2002**, *295*, 2400–2403. (b) Reinhoudt, D. N.; Crego-Calama, M. *Science* **2002**, *295*, 2403–2407. (c) Kato, T. *Science* **2002**, *295*, 2414–2418. (d) Whitesides, G. M.; Grybowski, B. *Science* **2002**, *295*, 2418–2421.

(15) (a) Barber, J.; Andersson, B. *Nature* **1994**, *370*, 31–34. (b) Gust, D.; Moore, T. A.; Moore, A. L. *Acc. Chem. Res.* **2001**, *34*, 40–48. (c) Wasielewski, M. R. *J. Org. Chem.* **2006**, *71*, 5051–5066. (d) Armaroli, N.; Balzani, V. *Angew. Chem., Int. Ed.* **2007**, *46*, 52–66.

(16) (a) Jenekhe, S. A. *Chem. Mater.* **2004**, *16*, 4381–4846. (b) Wassel, R. A.; Gorman, C. B. *Angew. Chem., Int. Ed.* **2004**, *43*, 5120–5123. (c) Carroll, R. L.; Gorman, C. B. *Angew. Chem., Int. Ed.* **2002**, *41*, 4378–4400.

(17) (a) Lehn, J.-M. *Science* **2002**, *295*, 2400–2403. (b) Kato, T.; Mizoshita, N.; Kishimoto, K. *Angew. Chem., Int. Ed.* **2006**, *45*, 38–68. (c) Hahn, U.; Elhabiri, M.; Trabolsi, A.; Herschbach, H.; Emmanuelle Leize, E.; Van Dorsselaer, A.; Albrecht-Gary, A.-M.; Nierengarten, J.-F. *Angew. Chem., Int. Ed.* **2005**, *44*, 5338–5341.

(18) (a) Sijbesma, R. P.; Beijer, F. H.; Brunsveld, L.; Folmer, B. J. B.; Hirschberg, J. H.; K, K.; Lange, R. F. M.; Lowe, J. K. L.; Meijer, E. W. *Science* **1997**, *278*, 1601–1604. (b) Hirschberg, J. H. K. K.; Brunsveld, L.; Ramzi, A.; Vekemans, J. A. J. M.; Sijbesma, R. P.; Meijer, E. W. *Nature* **2000**, *407*, 167–170. (c) Brunsveld, L.; Folmer, B. J. B.; Meijer, E. W.; Sijbesma, R. P. *Chem. Rev.* **2001**, *101*, 4071–4097. (d) Sánchez, L.; Martín, N.; Guldi, D. M. *Angew. Chem., Int. Ed.* **2005**, *44*, 5374–5382.

(19) (a) Hofmeier, H.; Schubert, U. S. *Chem. Commun.* **2005**, 2423–2432. (b) Chow, C.-F.; Fujii, S.; Lehn, J.-M. *Angew. Chem., Int. Ed.* **2007**, *46*, 5007–5010.

(20) (a) Miyauchi, M.; Takashima, Y.; Yamaguchi, H.; Harada, A. *J. Am. Chem. Soc.* **2005**, *127*, 2984–2989. (b) Miyauchi, M.; Harada, A. *J. Am. Chem. Soc.* **2004**, *126*, 11418–11419.

(21) (a) Yamashita, Y.; Kobayashi, Y.; Miyashi, T. *Angew. Chem., Int. Ed. Engl.* **1989**, *28*, 1052–1053. (b) Bryce, M. R.; Moore, A. J.; Hasan, M.; Ashwell, G. J.; Fraser, A. T.; Clegg, W.; Hursthouse, M. B.; Karaulov, A. I. *Angew. Chem., Int. Ed. Engl.* **1990**, *29*, 1450–1452. (c) Martín, N.; Sánchez, L.; Seoane, C.; Ortí, E.; Viruela, P. M. *J. Org. Chem.* **1998**, *63*, 1268–1279. (d) Segura, J. L.; Martín, N. *Angew. Chem., Int. Ed.* **2001**, *40*, 1372–1409.

(22) (a) Martín, N. *Chem. Commun.* **2006**, 2093–2104. (b) Guldi, D. M.; Zerbetto, F.; Georgakilas, V.; Prato, M. *Acc. Chem. Res.* **2005**, *38*, 38–43. (c) Vostrowsky, O.; Hirsch, A. *Angew. Chem., Int. Ed.* **2004**, *43*, 2326–2329. (d) Echegoyen, L.; Echegoyen, L. E. *Acc. Chem. Res.* **1998**, *31*, 593–601. (e) Martín, N.; Sánchez, L.; Illescas, B. M.; Pérez, I. *Chem. Rev.* **1998**, *98*, 2527–2548.

(23) (a) Pérez, E. M.; Sánchez, L.; Fernández, G.; Martín, N. *J. Am. Chem. Soc.* **2006**, *128*, 7172–7173. (b) Pérez, E. M.; Sierra, M.; Sánchez, L.; Torres, M. R.; Viruela, R.; Viruela, P. M.; Ortí, E.; Martín, N. *Angew. Chem., Int. Ed.* **2007**, *46*, 1847–1851. (c) Fernández, G.; Pérez, E. M.; Sánchez, L.; Martín, N. *Angew. Chem., Int. Ed.* **2008**, *47*, 1094–1097. (d) Fernández, G.; Pérez, E. M.; Sánchez, L.; Martín, N. *J. Am. Chem. Soc.* **2008**, *130*, 2410–2411.

(24) For a recent review on covalent C_{60}-TTF based dyads, see: Martín, N.; Sánchez, L.; Herranz, M. A.; Illescas, B. M.; Guldi, D. M. *Acc. Chem. Res.* **2007**, *40*, 1015–1024.

(25) Pristine exTTF molecule has been demonstrated to be unable to recognize fullerene or some of its derivatives like PCBM either in solution (see ref 23a) or in solid state; see: Otero, R.; Écija, D.; Fernández, G.; Gallego, J. M.; Sánchez, L.; Martín, N.; Miranda, R. *Nano Lett.* **2007**, *7*, 2602–2607.

Scheme 1. Synthesis of G2 to G4 exTTF-Based Dendrimers and the Previously Reported G0 and G1 Congeners

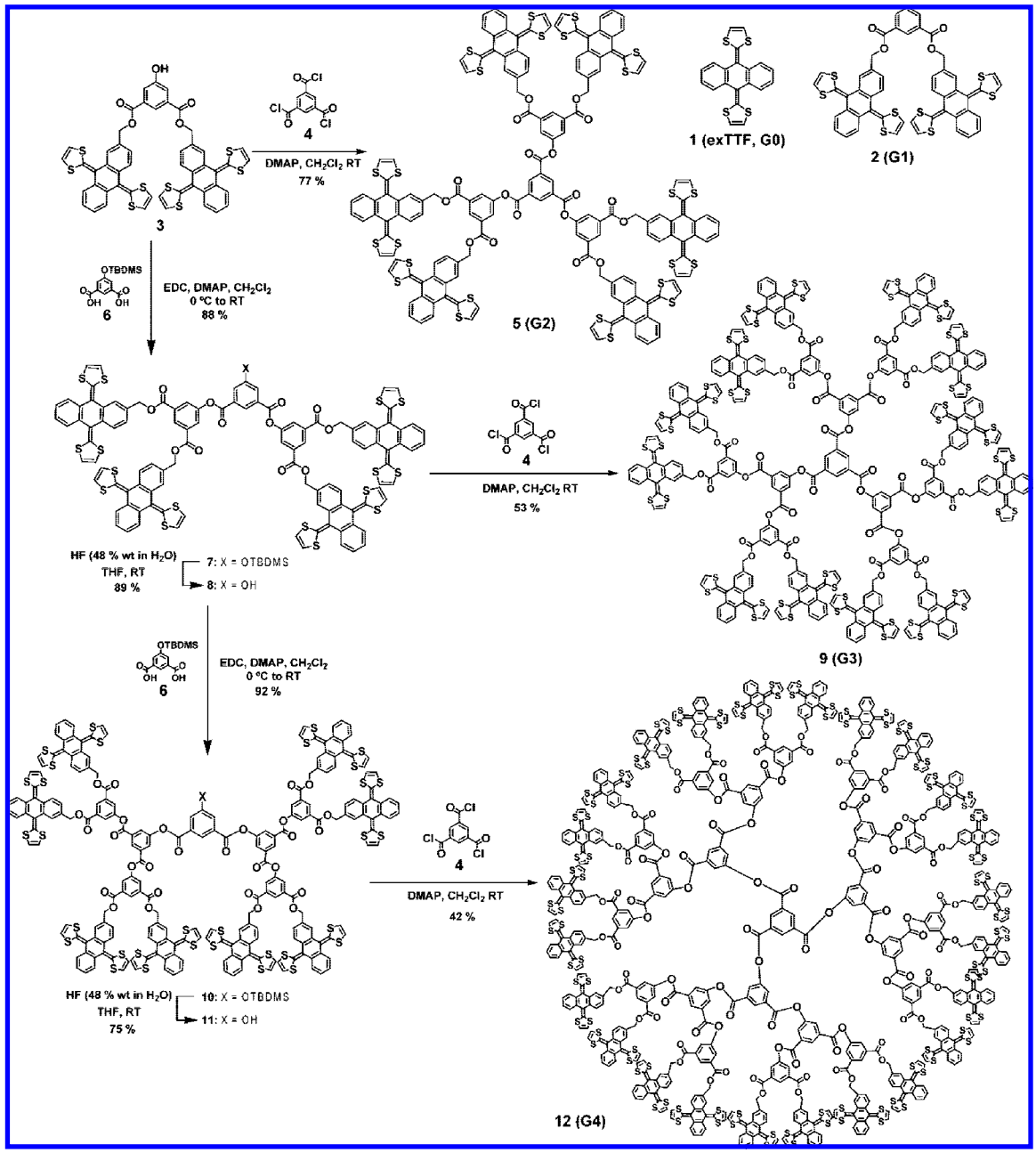

deprotection of the resulting dendron, and subsequent esterification with **4**.

Unlike in the previous work by Godbert and Bryce,[9c] in which the authors were unable to synthesize higher generation analogues of exTTF-based dendrimers due to the unfruitful attempts to deprotect the dendron wedge endowed with eight exTTF fragments, we have achieved the elimination of the protecting silyl group of dendronized building block **10** with a 500-fold excess of hydrofluoric acid. From **10** and again by a 3-fold esterification protocol with acid chloride **4** we have prepared G4 dendrimer **12**, bearing 24 exTTF moieties, in a 42% yield (see Supporting Information).

Dendrimers **5**, **9**, and **12**, together with their corresponding dendronized precursors, have been characterized by ^{1}H and ^{13}C NMR, FTIR, UV−vis, and MALDI-TOF (matrix assisted laser desorption ionization-time-of-flight) mass spectrometry (see Supporting Information). UV−vis spectra of dendrimers from G0 to G4 ($CHCl_3$, 298 K) show the augmentation of the absorption of all dendrimers with increasing generation and correspond to the product of the extinction coefficient of G0 by the number of exTTF units present in the final dendrimer (Figure 1). Plotting the extinction coefficient, at two different wavelengths (365 and 434 nm), against the number of exTTF units shows a linear fitting passing through the origin that supports the flawless regularity of all the final compounds synthesized (see inset in Figure 1).

The ^{1}H NMR spectrum of dendrimer **5** shows only one set of resonances (see Supporting Information). The sharp singlets at $\delta \approx 9.1$, 8.8, and 8.2, corresponding to the different isophthalic spacers, and at $\delta \approx 5.4$, assigned to the methylene

(26) Miller, T. M.; Kwok, E. W.; Neenan, T. X. *Macromolecules* **1992**, *25*, 3143–3148.

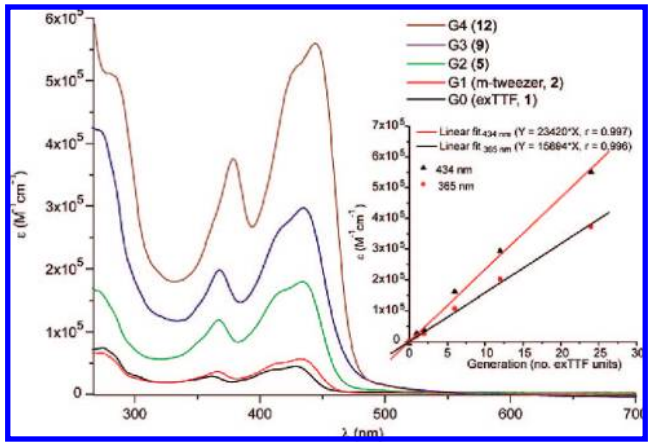

Figure 1. Comparison of absorption spectra of dendrimers **1**, **2**, **5**, **9**, and **12**, i.e. from the zeroth to fourth generation ($CHCl_3$, 298 K). The inset shows the plot of number of exTTF units in dendrimers vs absorbance at 365 and 434 nm.

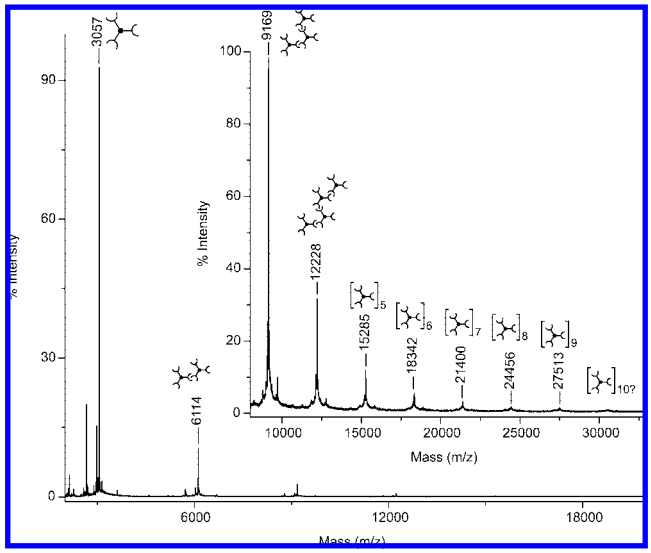

Figure 2. MALDI-TOF (ditranol) mass spectrum of dendrimer **5**. The inset shows the formation of oligomers up to the nonamer in the gas phase.

bridges that connect the peripheral exTTF fragments to the dendritic core, clearly support the regularity and C_{3v} symmetry of dendrimer **5**. In the case of **9**, the large number of exTTF units in the exterior of the dendrimer not only produces the broadening of the ^{1}H NMR resonances but also results in the presence of as many as five singlets of different intensity in the range 9−8 ppm. These findings suggest that the large size of each dendron wedge results in a significant loss of symmetry, and thus to the unisochronous behavior for these protons (see Supporting Information).

Despite dendrimer **12** showing limited solubility (≤0.2 mM) in most common organic solvents, we were able to register its ^{1}H and ^{13}C NMR spectra (DMSO-d_6, 343 K). The ^{1}H spectrum shows broad signals which follow the same pattern observed for its lower generation congener **9**.

Self-Assembly. The characterization of dendrimer **5** by MALDI-TOF mass spectrometry, using dithranol as matrix, allows the observation of the molecular ion peak corresponding to the isolated dendrimer (m/z = 3057) (Figure 2 and Figure S-1). We also observed ion peaks up to the nonamer (m/z = 27 513) indicative of the self-assembly of dendrimer **5** into large aggregates in the gas phase. Although the possibility of intramolecular $\pi-\pi$ interactions among the exTTF units of analogue dendrimers has been previously mentioned,[9c] to the best of our knowledge, this is the first example of intermolecular aggregation of exTTF-based systems to form supramolecular dendritic aggregates in which the binding motifs are the sum of numerous $\pi-\pi$ aromatic interactions between the exTTF units, despite their butterfly-like shape highly distorted from planarity.[21] The MALDI-TOF mass spectrum of compound **9** showed, in addition to the molecular peak of the isolated dendrimer (m/z = 6398), another peak at m/z = 12 796, corresponding to the dimer and broad signals centered at m/z values around 18 000 and 21 000 which match with the formation of large supramolecular clusters of dendrimers (Figure S-2).

Evidence of the self-assembly of exTTF-based dendrimers in solution has been achieved by concentration dependent (CD) and variable temperature (VT) ^{1}H NMR experiments performed in 0.3−10 mM solutions of G2 and G3 dendrimers in $CDCl_3$. As in the previous supramolecular architectures reported by our research group as well as in previous studies performed for related supramolecular ensembles,[23,27] in the CD-^{1}H NMR experiments the increase in the concentration results in the slight downfield shift and broadening of most resonances (Figure 3a and S-3a). Regarding the VT-^{1}H NMR experiments, those spectra registered at 298 K or above show the presence of sharp resonances which is diagnostic of a low self-assembly degree. The trend observed—upfield shift of aromatic signals together with the shield to low fields experimented by the 1,3-dithiole rings—agrees with the interaction of the anthracene-like units to form the aggregates of dendrimers (Figure 3b and S-3b). Besides these shifts, all the ^{1}H NMR signals experience a slight broadening as temperature decreases. Although this is generally regarded as indicative of self-assembly, taking into account the high molecular weight of our dendrimers, it is difficult to assess whether this broadening is due to the formation of noncovalent architectures or simply the slow down of the relaxation kinetics.

Several attempts to obtain an accurate MALDI-TOF spectrum of **12** have resulted in the observation of a big lump at around 13 000 units of atomic mass indicative of the presence of the proposed structure (see Figure S-4). Unfornutalely, the low solubility of G4 dendrimer **12** has also prevented the investigation of its self-assembly process to form aggregates by variable concentration ^{1}H NMR spectroscopy.

A definitive proof for the self-assembly of dendrimers **5**, **9**, and **12** in solution was obtained by dynamic light scattering in chloroform (Figure 4). These measurements showed a narrow distribution of aggregates with calculated hydrodynamic radii (R_H) that ranges from ∼30 nm for second generation **5** to ∼60 nm for third generation **12** and to ∼120 nm for fourth generation **12**. These values for R_H indicate the aggregation in solution of around 10 molecules of **5**, 12 of **9**, and 20 of **12**, respectively.

The formation of large clusters of dendrimers on the surface has been visualized by atomic force microscopy (AFM) on mica. Figure 5 shows the aggregates of dendrimers **5**, **9**, and **12** after dropcasting (sub)micromolar solutions of these compounds in chloroform. The adsorption of all dendrimers reported, from G2 to G4, results in the formation of semispherical objects with different diameters and heights depending on the generation. For the case of **5**, the particles present an average diameter of

(27) Haino, T.; Matsumoto, Y.; Fukazawa, Y. *J. Am. Chem. Soc.* **2005**, *127*, 8936–8937.

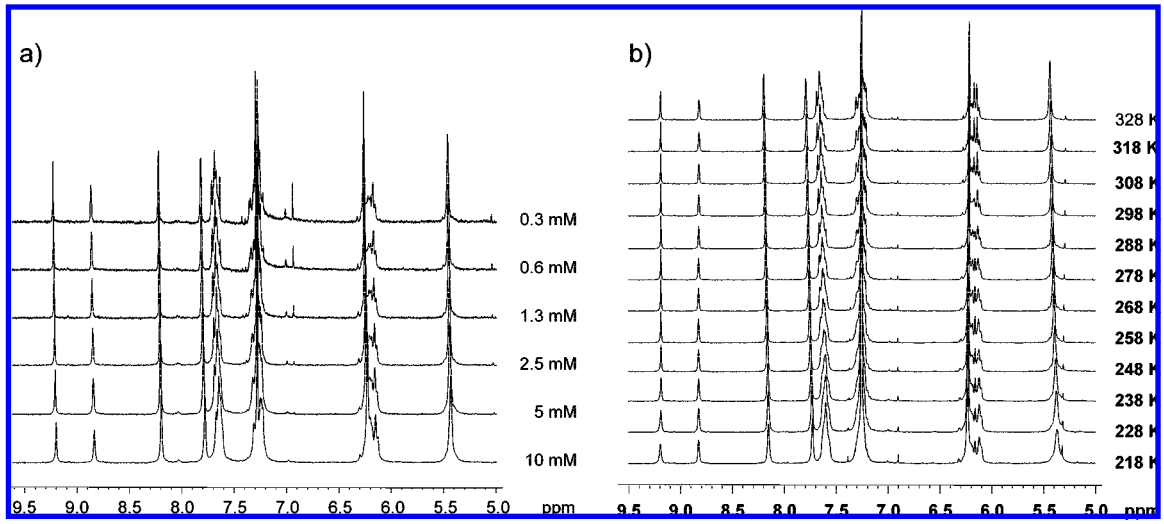

Figure 3. Partial ^{1}H NMR spectra ($CDCl_3$, 300 MHz) of **5** at different concentrations at 298 K (a) and at variable temperature (b) showing the aromatic region, the 1,3-dithiole rings, and the exTTF methylenes.

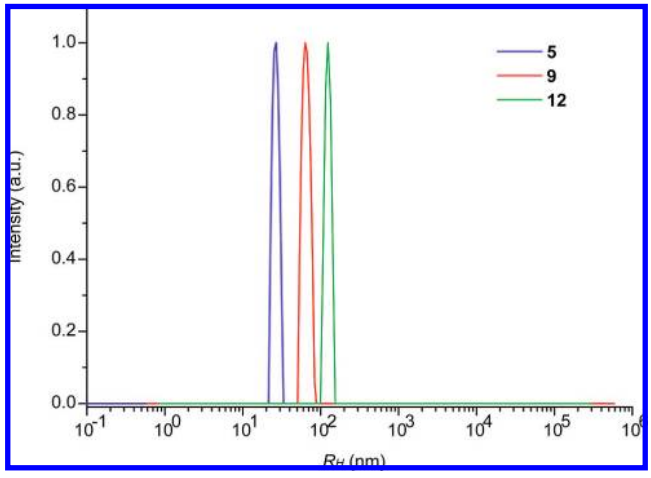

Figure 4. Normalized distribution of hydrodynamic radii (R_H) of aggregates of **5**, **9**, and **12** ($CHCl_3$, 2.0×10^{-4} M, 298 K).

~170 nm. G3 dendrimer **9** forms a larger number of clusters than that observed for **5** (Figure 5b), and unlike G2, the average diameter is lower with values of ~130 nm. As expected, the associates formed on surface are larger than those found in solution by DLS.

A further proof for the self-assembly of third generation dendrimer **9** has been obtained by the scanning electron microscopy (SEM) images (Figure S-5). The SEM images of compound **9** show a pseudoglobular shape for the self-assembled particles with diameters larger than 100 nm. These values are in good accordance with those previously obtained by AFM.

The low concentration required for AFM imaging has allowed us to visualize the formation of G4-based clusters (Figure 5c). These objects show lower diameter sizes than those of its lower generation congeners (90 nm). The decrease in size of the associates on a solid support with increasing generation is most likely a direct consequence of the decrease in solubility from **5** to **9** to **12**, which accelerates precipitation. In fact, the size of the clusters formed by **12** on mica is nearly identical to that found in solution.

The height profiles of the clusters shed values of approximately 15 nm for **5** and **9**, whereas for **12** this value is around 10 nm. The poor availability of all peripheral exTTF units to interact with other units of different congeners, most probably due to its highly distorted geometry, could justify the size features, regarding the diameter and height of the clusters, observed for **12**. The height values obtained for all the compounds studied are indicative of the stacking of a number of dendrimeric units (Figure 5d−f). With regards to the three-dimensional AFM images (Figure 5g−i), in all cases, disk-like shapes are observed for the resulting clusters instead of the expected more globular ones predicted by theoretical calculations (see Figure S-6).[28] This change in geometry, due to the flattening and distortion effects undergone by a number of dendrimers in contact with surfaces of different nature, is a well-documented phenomenon.[29]

All the above experimental evidence supports the self-assembly of the dendrimers reported herein by a combination of aromatic $\pi-\pi$ aromatic stacking interactions and van der Waals forces.

Peripheral Multiencapsulation of C_{60}. A challenging task for the systems presented in this work is the formation of supramolecular arrays of donor and acceptor units with the long-term goal of preparing suitable complementary electroactive candidates for the fabrication of optoelectronic devices.[24] With this objective in mind, we have taken advantage of the ability of our in-house tweezer receptor (G1 dendrimer, **2**) to complex C_{60},[23a] and we have investigated the peripheral binding of [60]fullerene by dendrimers **5**, **9**, and **12**.

The ability of **5** to host C_{60} has been evaluated by UV−vis titration in chlorobenzene as solvent.[30] Figure 6 depicts the changes observed in the electronic spectrum of **5**, **9**, and **12** (6.1×10^{-6} M, 298 K) upon addition of growing amounts of a C_{60} solution (4.2×10^{-3} M, 298 K) in chlorobenzene. As in

(28) *HyperChem*, release 7.51; HyperCube Inc.: Gainesville, FL, 2002.
(29) (a) Hermans, T. M.; Broeren, M. A. C.; Gomopoulos, N.; Smeijers, A. F.; Mezari, B.; Van Leeuwen, E. N. M.; Vos, M. R. J.; Magusin, P. C. M. M.; Hilbers, P. A. J.; Van Genderen, M. H. P.; Sommerdijk, N. A. J. M.; Fytas, G.; Meijer, E. W. *J. Am. Chem. Soc.* **2007**, *129*, 15631–15638. (b) Tsukruk, V. V.; Rinderspacher, F.; Bliznyuk, V. N. *Langmuir* **1997**, *13*, 2171–2176. (c) Li, J.; Swanson, D. R.; Qin, D.; Brothers, H. M.; Piehler, L. T.; Tomalia, D.; Meier, D. J. *Langmuir* **2000**, *15*, 7347–7350.
(30) UV−vis titration of the first generation dendrimer **2** in chlorobenzene has proven the ability of this receptor to act as a tweezer-like host binding one C_{60} molecule. See ref 23a.

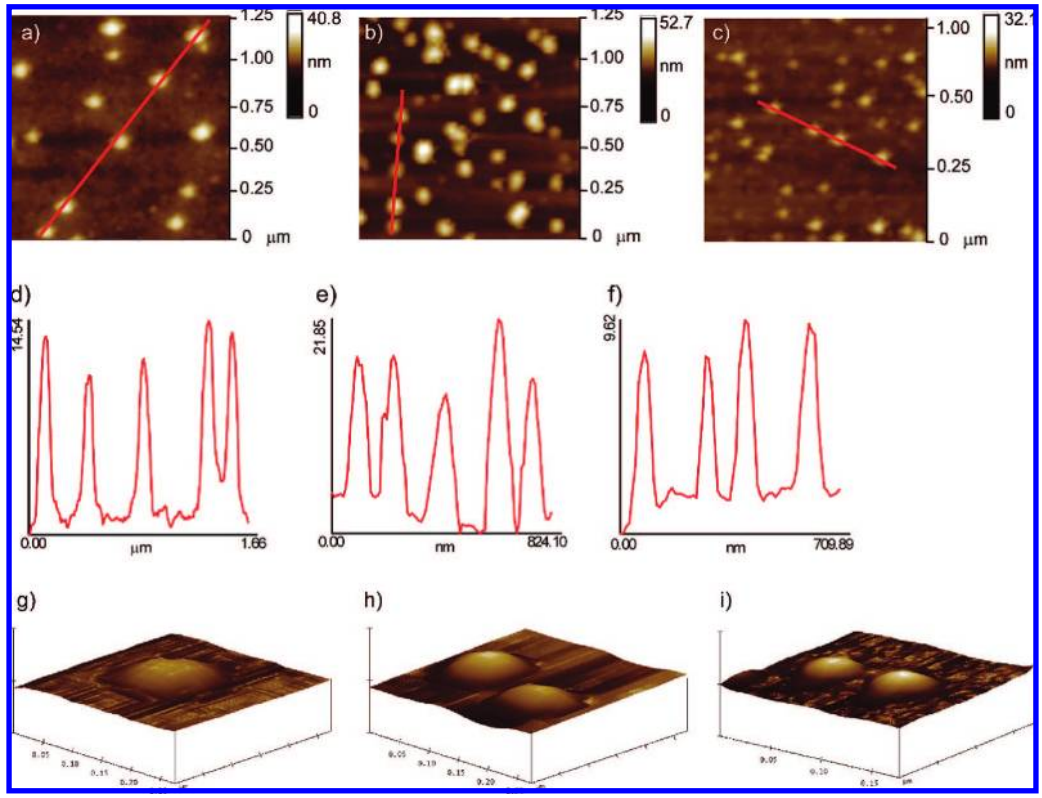

Figure 5. AFM images (tapping mode, air, 298 K) of dropcast of chloroform solutions of **5** (a), **9** (b), and **12** (c) on mica. (d−f) Height profiles along the red lines depicted in the corresponding figures for dendrimers **5**, **9**, and **12**, respectively. (g−i) Images illustrating the disk-like geometry observed for all the dendrimers.

our previous studies,[23] the decrease in the intensity of the maximum at $\lambda = 437$ nm is accompanied by the apparition of a new band—diagnostic of a charge transfer interaction—at $\lambda = 483$ nm that increases in intensity at higher C_{60} concentration. The lack of an isosbestic point during this titration experiment points to the coexistance of **5**·C_{60} complexes of several different stoichiometries.

Interestingly, this binding process occurs in a positive cooperative manner as it has been demonstrated by plotting the absorption changes at $\lambda = 437$ nm against the concentration of C_{60}. The obtained binding isotherm is sigmoidal in shape with a good fitting ($R^2 = 0.998$) to the Hill equation.[31] The calculated values for the apparent binding constant (K_{app}) and for the Hill coefficient are (2238 ± 33) M^{-1} and 2.6 ± 0.1, respectively. The tweezer-like behavior of all the three dendron wedges constitutive of **5** together with the Hill coefficient (the upper limit should be 3) suggests the complexation of three C_{60} molecules per dendrimer via a highly cooperative mechanism.[23a,32] Several attempts to further confirm that stoichiometry have been carried out by means of Job's plots at different concentrations (10^{-5} to 10^{-4} M). The complex results obtained for these experiments suggest the presence of complexes of different stoichiometric ratios most likely due to the need of disrupting the dendrimer-based aggregates prior to the complexation of C_{60} which prevents the unambiguous determination of the final complex stoichiometry.

UV−vis titration experiments carried out with **9** and **12** show similar features to those observed for **5**, that is, the depletion of the maximum at $\lambda = 437$ nm and the increase of the charge-transfer band at ∼487 nm (Figure 6). The analysis of the complexation process of these high generation dendrimers with C_{60} gives rise to sigmoidal isotherms for both **9** and **12** with apparent association constants of (3085 ± 33) and (2137 ± 21) M^{-1}, respectively. The calculated Hill coefficient is 2.7 ± 0.1 for **9** and 3.4 ± 0.1 for **12**, which indicates a similar degree of cooperativity in the binding events. Most probably, the cooperative effect arises from the need to disassemble the dendrimers prior to complexation of C_{60}.

The complexation of C_{60} by **5** and **9** has been corroborated by ^{1}H NMR studies (Figure S-7). The shifting pattern observed for first generation dendrimer **2** and other related exTTF-based receptors upon complexation of [60]fullerene is also seen in these NMR studies.[23] Thus, the aromatic resonances experience an upfield shift, and at the same time, those corresponding to the 1,3-dithiole rings slightly shift downfield. The former behavior is justified by considering the binding of C_{60} based on the aromatic size of the exTTF moieties, and the latter is indicative of the charge transfer process—observed in the UV−vis experiments as well—undergone between the electronically complementary host and guest.

(31) The applicability of the Hill equation to small molecule self-assembling systems has recently been under discussion. In a careful analysis, G. Ercolani (Ercolani, G. *J. Am. Chem. Soc.* **2003**, *125*, 16097–16103) has argued in favor of the use of the Hill equation only for intermolecular binding of monovalent ligands to a multivalent receptor. Our proposed binding mode fits with this case, since the binding of C_{60} always occurs intermolecularly

(32) Although it is often considered a direct indication of the number of available binding sites on the receptor, the Hill coefficient is best thought of as an interaction coefficient reflecting the extent of cooperativity, with a maximum value equal to the number of binding sites (see: Connors, K. A. *Binding Constants*; John Wiley & Sons: New York, 1987).

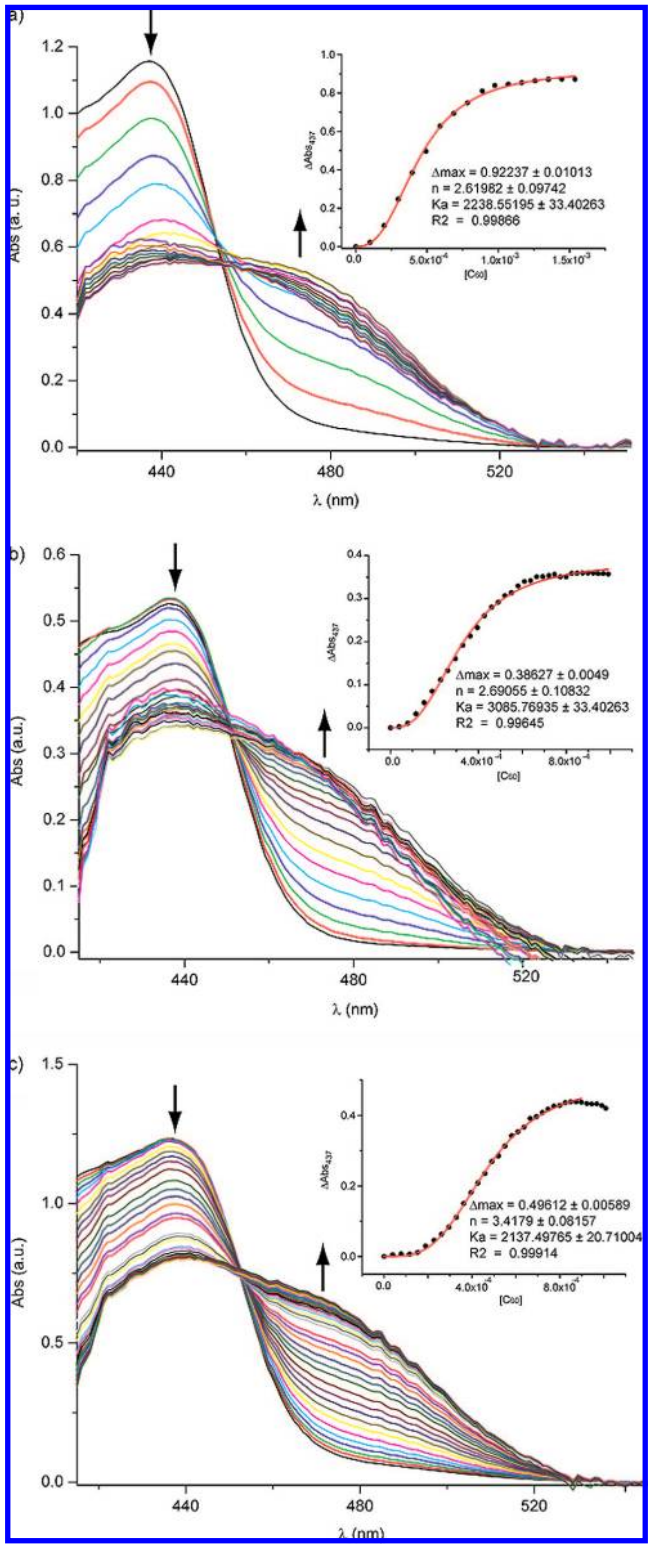

Figure 6. Absorption spectral changes of dendrimers **5** (chlorobenzene, 298 K, 6.1×10^{-5} M) (a), **9** (chlorobenzene, 298 K, 1.3×10^{-5} M) (b), and **12** (chlorobenzene, 298 K, 2.2×10^{-5} M) (c) upon addition of fullerene (chlorobenzene, 298 K, 4.1×10^{-3} M). The absorption spectra of fullerene have been subtracted. The inset shows the fit of ΔAbs (437 nm) to the Hill equation.

Redox Properties. The dense electron-rich periphery of dendrimers **5**, **9**, and **12** could result in a multielectron oxidation process in which *n* identical exTTF moieties, which are able to donate two electrons each, gives rise to a single wave involving

Table 1. Redox Potentials and Diffusion Coefficients of Compounds **1**, **2**, and the New Dendrimers (**5**, **9**, and **12**)

compd	E^1_{ox}[a]	D[b] ($cm^2\ s^{-1}$)
1	+0.25	8.87×10^{-6}
2	+0.22	5.28×10^{-6}
5	+0.27 (+0.15)[c]	2.81×10^{-6}
9	+0.27 (+0.14)[c]	1.44×10^{-6}
12	+0.32 (+0.14)[c]	0.44×10^{-6}

[a] Experimental conditions: V vs $Ag/AgNO_3$, oDCB/CH_3CN (4:1) as solvent, GCE as working electrode, Pt as counter electrode, Bu_4NClO_4 (0.1 M) as supporting electrolyte; scan rate 50 mV s^{-1}. [b] Experimental conditions: V vs $Ag/AgNO_3$, oDCB/CH_3CN (4:1) as solvent, GCE as working electrode, Pt as counter electrode, Bu_4NClO_4 (0.1 M) as supporting electrolyte; step potential 0.7 V. [c] Associated to an adsorption process.

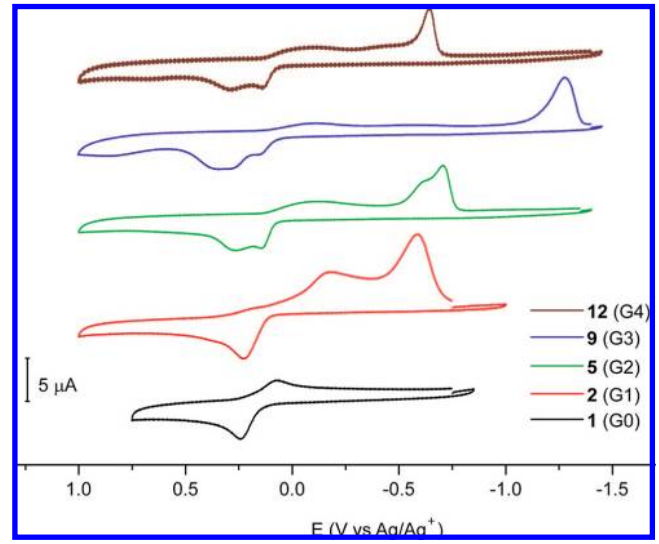

Figure 7. Cyclic voltammograms of the dendrimers reported from the zeroth to fourth generation. All the measurements have been carried out in oDCB/MeCN (4:1), 298 K, at total concentration ~0.125 mM of electroactive species, utilizing Bu_4NClO_4 (0.1 M) as supporting electrolyte, a glassy carbon as working electrode, and at 50 mV/s as scan rate.

$2 \times n$ electrons (this is the case for **1** and **2**) or, alternatively, the coulombic repulsion among the cations produced by the sequential oxidation of these units could lead to separated waves with close oxidation potentials.

The redox behavior of all the dendrimers, from the zeroth to fourth generation, has been investigated by cyclic voltammetry in oDCB/MeCN (4/1) as solvent and is shown in Table 1 and Figure 7. Whereas compounds **1** and **2** present only one oxidation wave, dendrimer **5** shows two broad oxidation waves as a consequence of either the mentioned coulombic repulsion among the peripheral exTTF units or, most probably, a weak adsorption phenomenon of the substrate on the electrode surface (see below). In all cases, the oxidation process is electrochemically irreversible, and the reduction of the positively charged species appears at different potential values depending on the generation. The same trend is also observed for dendrimers **9** and **12** (see Table 1).

The potential application of dendrimers in different research fields like catalysis[3] or drug realease[5] requires the study of the diffusion of these large monodisperse molecules in solution. Different electrochemical techniques can be utilized to measure

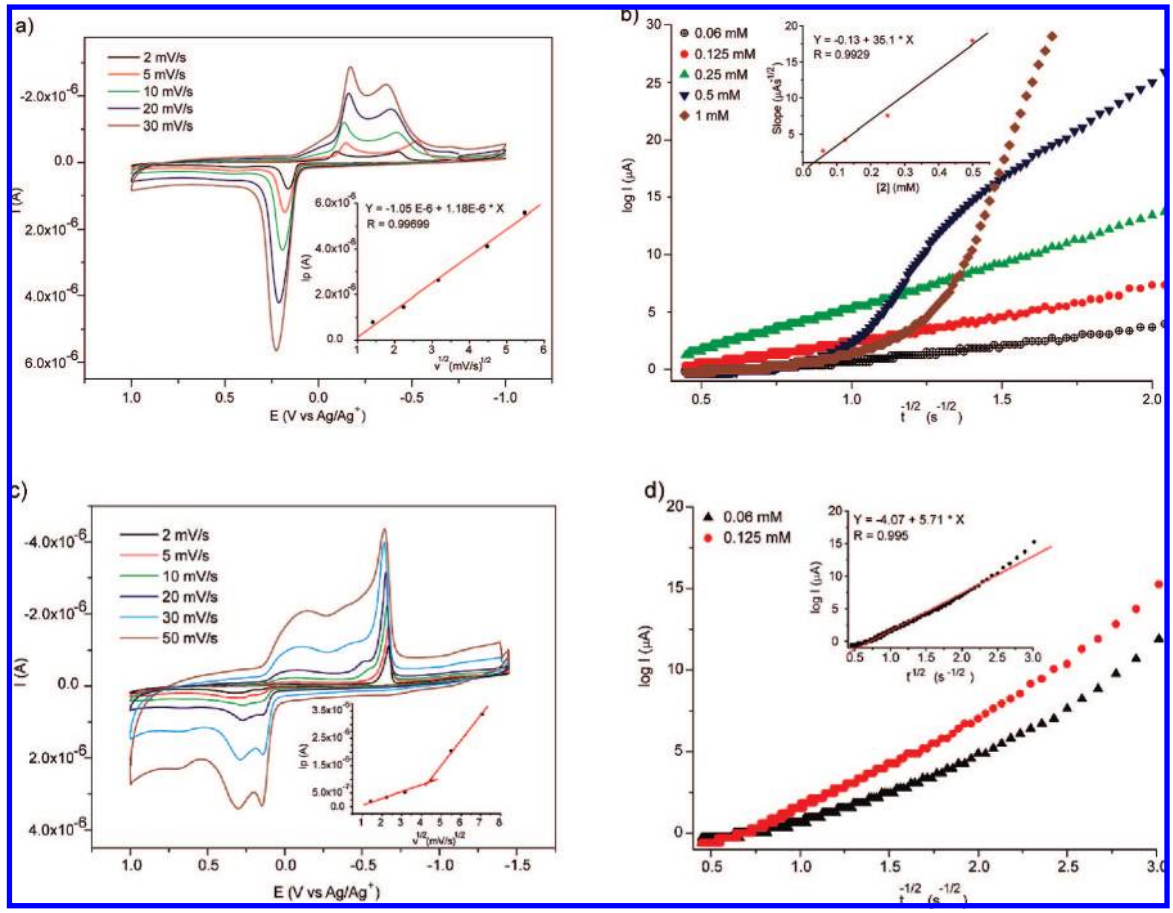

Figure 8. Cyclic voltammograms of **2** (a) and **12** (c) (~0.125 mM) at different scan rates. The inset in (a) and (c) show the plot of the current intensity against the square root of the scan rate for **2** and **12**, respectively. Linearized current−time plots obtained from the chronoamperograms of **2** (b) and **12** (d and inset) at different concentrations and at potential step of 0.7 V. The inset in (b) shows the slope of the straight lines vs the concentration of **2**. All the measurements have been carried out in oDCB/MeCN (4:1), 298 K, Bu_4NClO_4 (0.1 M) as supporting electrolyte and a glassy carbon as working electrode.

the diffusion coefficient (D) of redox-active dendrimers.[33] Herein, we have used cyclic voltammetry and chronoamperommetry techniques for the determination of the diffusion coefficient of the dendrimers, from the zeroth to fourth generation. For compounds **1** and **2**, the oxidation currents increase linearly with the square root of the sweep rate (Figure 8a and Figures S-8 and S-9) which implies that the electrochemical process is controlled by diffusion. Nonetheless, for compounds **5**, **9**, and **12** (Figure 8c) the current intensity is only linearly proportional to the square root of the scan rate at low values of this parameter, whereas at high values of the scan rate the current intensity becomes directly proportional to the scan rate. These findings can be justified by considering a weak adsorption of the substrates on the surface of the electrode and could account for the oxidation postwave observed in the cyclic voltammograms (Figure 8c).[34]

To determine the diffusion coefficient, we have performed a series of chronoamperometric measurements in solutions of different concentrations (Table 1). In all cases, the electrode potential has been fixed at 0.7 V. From these experiments and by using the Cottrell equation (eq 1)—where n is the number of electrons, A is the surface area of the working electrode, and C is the concentration of the substrate (in mol cm^{-3})—we can deduce the diffusion coefficient.[34]

$$I = nFAC\sqrt{\frac{D}{\pi t}} \qquad (1)$$

For the case of exTTF (**1**), the linearized current−time transients result in straight lines for all the concentration range used (0.06 mM to 1 mM) (Figure S-8). The slopes of those straight lines were plotted versus the concentration of **1**, and the combined use of the slope and the Cottrell equation leads to a diffusion coefficient value of 8.8×10^{-6} cm^2 s^{-1} (Table 1).[35] A similar chronoamperometric analysis for the tweezer **2** shed straight lines for the concentration values ranging from 0.06 to 0.25 mM (Figure 8b) and a calculated value of 5.28×10^{-6} cm^2 s^{-1} for D (Table 1). However, at 0.5 and 1 mM the Cottrell plot leads to curved lines that could be justified by considering the adsorption and/or the self-aggregation processes.

The chronoamperograms of higher generation dendrimers **5** and **9** provided similar results. As shown in Figure S-9, at low concentration values (0.06 and 0.125 mM) one can observe straight lines in the linearized current−time plots, whereas at higher concentration curved Cottrell plots appear (Figure S-9).

(33) Golsmith, J. I.; Takada, K.; Abruña, H. D. *J. Phys Chem. B* **2002**, *106*, 8505–8513.
(34) *Electrochemical Methods. Fundamentals and Applications*; Bard, A. J., Faulkner, L. R., Eds.; John Wiley & Sons: 2001.
(35) To the best of our knowledge, this is the first value reported for the diffusion coefficient for the well-known exTTF **1**.

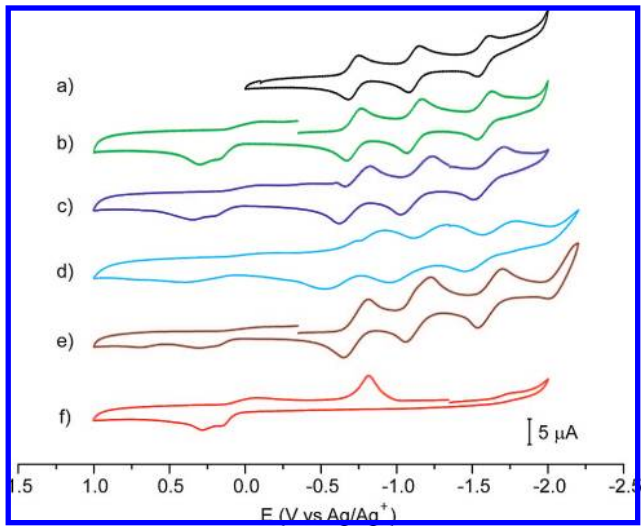

Figure 9. Cyclic voltammograms of C_{60} (a), **5** (f), and the successive additions of 1 (b), 2 (c), 3 (d), and 4 equiv (e) of fullerene (b−e). All the measurements have been carried out in oDCB/MeCN (4:1), 298 K, at total concentration of **5** of ∼0.125 mM, utilizing Bu_4NClO_4 (0.1 M) as supporting electrolyte, 50 mV/s as scan rate, and a glassy carbon as working electrode.

Solubility issues have prevented the registration of the chronoamperograms of **12** at concentrations higher than 0.125 mM (Figure 8d). However, the chronoamperograms of **12** at 0.06 and 0.125 mM show a similar trend to that observed for **5** and **9** at these concentration values. In these three cases, we have used the I vs $t^{-1/2}$ plots at 0.125 mM to attain values for the diffusion coefficient of 2.81×10^{-6}, 1.44×10^{-6}, and 0.44×10^{-6} cm^2 s^{-1} for **5**, **9**, and **12** at 0.125 mM, respectively. As expected, the magnitude of D decreases with increasing dendrimer size (Table 1).[36]

Finally, we have investigated the effect that the peripheral complexation of **5** and **9** with C_{60} has on their redox properties, and those of C_{60}, by cyclic voltammetry in oDCB/MeCN (4/1) as solvent (Figure 9 and Figure S-10). The sequential addition of up to 3 equiv of C_{60} to a 0.125 mM solution of **5** results in the progressive broadening and a cathodic shift of the reduction waves corresponding to the fullerene. This effect is justified by considering the electron-rich environment close to the complexed C_{60} guests which makes its reduction process more energetic. The addition of a fourth equivalent of C_{60} results in sharper and more intense reduction waves at potential values close to that of the free fullerene. A plausible explanation for these findings can be that upon complexation of up to three C_{60} molecules per molecule of **5** the excess of fullerene, which has a higher D value,[37] masks those waves corresponding to the final complex.[38] A similar trend has been observed for **9** upon addition of more than 6 equiv of C_{60}. These experiments can be considered as an indirect proof of the stoichiometry of the fullerene dendrimer complexes.

Conclusions

The convergent synthesis of a set of dendrimers, up to the fourth generation, decorated in their periphery with exTTF moieties, which are well-known for their electron-donor features, is reported. Despite the butterfly-like geometry of the exTTF units, all the dendrimers have been demonstrated to self-assemble into clusters of several dendritic units. The self-aggregation process is clearly supported, in the gas phase, by MALDI-TOF and, in solution, by variable temperature and concentration ^1H NMR experiments, respectively. Conclusive evidence for the self-assembly of dendrimers in solution has been obtained from DLS measurements, which reveal a relatively narrow distribution of aggregates and hydrodynamic radii ranging from ∼30 nm for **5** (G2) to ∼120 nm for **12** (G4). The self-assembly in the solid state was examined by AFM and SEM imaging. Typical AFM images show disk-like superstructures with height profiles of 15 nm for **5** and **9** and of 10 nm for **12**. On the surface, the trend in the diameters of the particles observed is opposed to that found in solution, increasing from **12** (100 nm) to **9** (130 nm) to **5** (170 nm), which is accounted for by the decrease in solubility with increasing generation, which promotes rapid precipitation and prevents further association of the higher generation dendrimers.

We have also investigated the self-diffusion of the molecules described by electrochemical methods. The diffusion coefficient, not only for the new dendrimers reported herein but also for the previously reported exTTF (**1**) and tweezer **2**, has been calculated from their chronoamperograms at different concentrations by means of the Cottrell equation. The calculated values for D were determined to be 8.8×10^{-6}, 5.28×10^{-6}, 2.81×10^{-6}, 1.44×10^{-6}, and 0.44×10^{-6} cm^2 s^{-1} for **1**, **2**, **5**, **9**, and **12**, respectively, thus demonstrating the decrease of this magnitude with increasing dendrimer size.

The geometrical and electronic complementarity of the peripheral exTTF units with the electron acceptor [60]fullerene allows dendrimers **5**, **9**, and **12** to host multiple C_{60} units, which could give rise to well-ordered donor−acceptor materials for the preparation of optoelectronic devices. The complexation process of C_{60} occurs in a positive homotropic cooperative manner as demonstrated by UV−vis titration experiments. The effect that complexation of C_{60} by **5** and **9** has on the redox properties of the parent compounds has also been explored by cyclic voltammetry. The successive addition of a number of equivalents of C_{60} to solutions of the dendrimers results in a broadening and a cathodic shift of the typical reduction waves of C_{60}.

We now plan to investigate the potential use of the donor−acceptor clusters in the preparation of optoelectronic devices like photovoltaic cells in which the order in the solid state is a key aspect to obtain improved morphologies in the search for higher energy conversion efficiencies.

Acknowledgment. Financial support by the MEC of Spain (Projects CTQ2005-02609/BQU and Consolider-Ingenio 2010C-07-25200) and the CAM (MADRISOLAR Project P-PPQ-000225-0505). G.F. thanks the MEC of Spain for a research grant, and E.M.P. is thankful for a Juan de la Cierva contract, cofinanced by the European Social Fund. We are thankful to A.

(36) For the sake of comparison we have determined D by pulse-field-gradient spin-echo NMR (PFGSE-NMR). The values obtained for **2**, **5**, and **9** are 3.05×10^{-6}, 1.74×10^{-6}, and 1.32×10^{-6} cm^2 s^{-1}, respectively. Unfortunately, the behavior of **12** under PFGSE-NMR conditions was found to be irregular which prevented the determination of D in this case.

(37) The diffusion coefficient of C_{60} has been calculated to be 14×10^{-6} cm^2 s^{-1}; see: Hishida, Y.; Nishi, M.; Baba, Y.; Ikeuchi, H. *Anal. Sci.* **2006**, *22*, 931–935.

Soubrié (Centro de Microscopía y Citometría, UCM) for AFM imaging, Dr. M. Alonso (UAM) for the MALDI-TOF spectra, and Dr. E. Saez and Dr. M[a] D. Molero for PFG-NMR experiments (CAI de RMN, UCM), and Unidad de Espectrocopía de Infrarrojo-Ramán-Correlación (UCM) for DLS experiments. We thank Dr. J. L. López, Dr. A. González, Prof. J. M. Pingarrón, and Prof. P. Yañez for their helpful discussions on the electrochemical measurements.

(38) The influence of the concentration of C_{60} on the cathodic shift of its reduction waves can be considered as negligible. Although this is the typical electrochemical behaviour for a reversible species (see ref 34), we have carried out the cyclic voltammograms of pristine C_{60} at different concentrations and no shift for the reduction waves are observed (see Figure S11).

Supporting Information Available: Experimental procedures with complete spectroscopic and structural analysis, including Supporting Figures S1−11. This material is available free of charge via the Internet at http://pubs.acs.org.

JA8018498